

## 1 **N<sub>2</sub>O-respiring bacteria in biogas digestates for reduced agricultural emissions**

2 Kjell Rune Jonassen<sup>1,3</sup>, Live H. Hagen<sup>1</sup>, Silas H.W. Vick<sup>1</sup>, Magnus Ø. Arntzen<sup>1</sup>,  
3 Vincent G.H. Eijsink<sup>1</sup>, Åsa Frostegård<sup>1</sup>, Paweł Lycus<sup>1</sup>, Lars Molstad<sup>4</sup>, Phillip B.  
4 Pope<sup>1,2</sup>, Lars R. Bakken<sup>1\*</sup>

5 <sup>1)</sup> Faculty of Chemistry, Biotechnology and Food Science, NMBU - Norwegian University of  
6 Life Sciences, 1432 Ås, Norway

7 <sup>2)</sup> Faculty of Biosciences, NMBU - Norwegian University of Life Sciences, Norway

8 <sup>3)</sup> VEAS WWTP, Bjerkåsholmen 125, 3470 Slemmestad, Norway.

9 <sup>4)</sup> Faculty of Science and Technology, Norwegian University of Life Sciences, Norway

10

11 \* corresponding author

## 12 **Abstract**

13 Inoculating agricultural soils with N<sub>2</sub>O-respiring bacteria (NRB) can reduce N<sub>2</sub>O-emissions, but would  
14 be impractical as a standalone operation. Here we demonstrate that digestates obtained after biogas  
15 production are suitable substrates and vectors for NRB. We show that indigenous NRB in digestates  
16 grew to high abundance during anaerobic enrichment under N<sub>2</sub>O. Gas-kinetics and meta-omic  
17 analyses showed that these NRB's, recovered as metagenome-assembled genomes (MAGs), grew by  
18 harvesting fermentation intermediates of the methanogenic consortium. Three NRB's were isolated,  
19 one of which matched the recovered MAG of a *Dechloromonas*, deemed by proteomics to be the  
20 dominant producer of N<sub>2</sub>O-reductase in the enrichment. While the isolates harbored genes required  
21 for a full denitrification pathway and could thus both produce and sequester N<sub>2</sub>O, their regulatory  
22 traits predicted that they act as N<sub>2</sub>O sinks in soil, which was confirmed experimentally. The isolates  
23 were grown by aerobic respiration in digestates, and fertilization with these NRB-enriched digestates  
24 reduced N<sub>2</sub>O emissions from soil. Our use of digestates for low-cost and large-scale inoculation with  
25 NRB in soil can be taken as a blueprint for future applications of this powerful instrument to engineer  
26 the soil microbiome, be it for enhancing plant growth, bioremediation, or any other desirable function.

## 27 **Introduction**

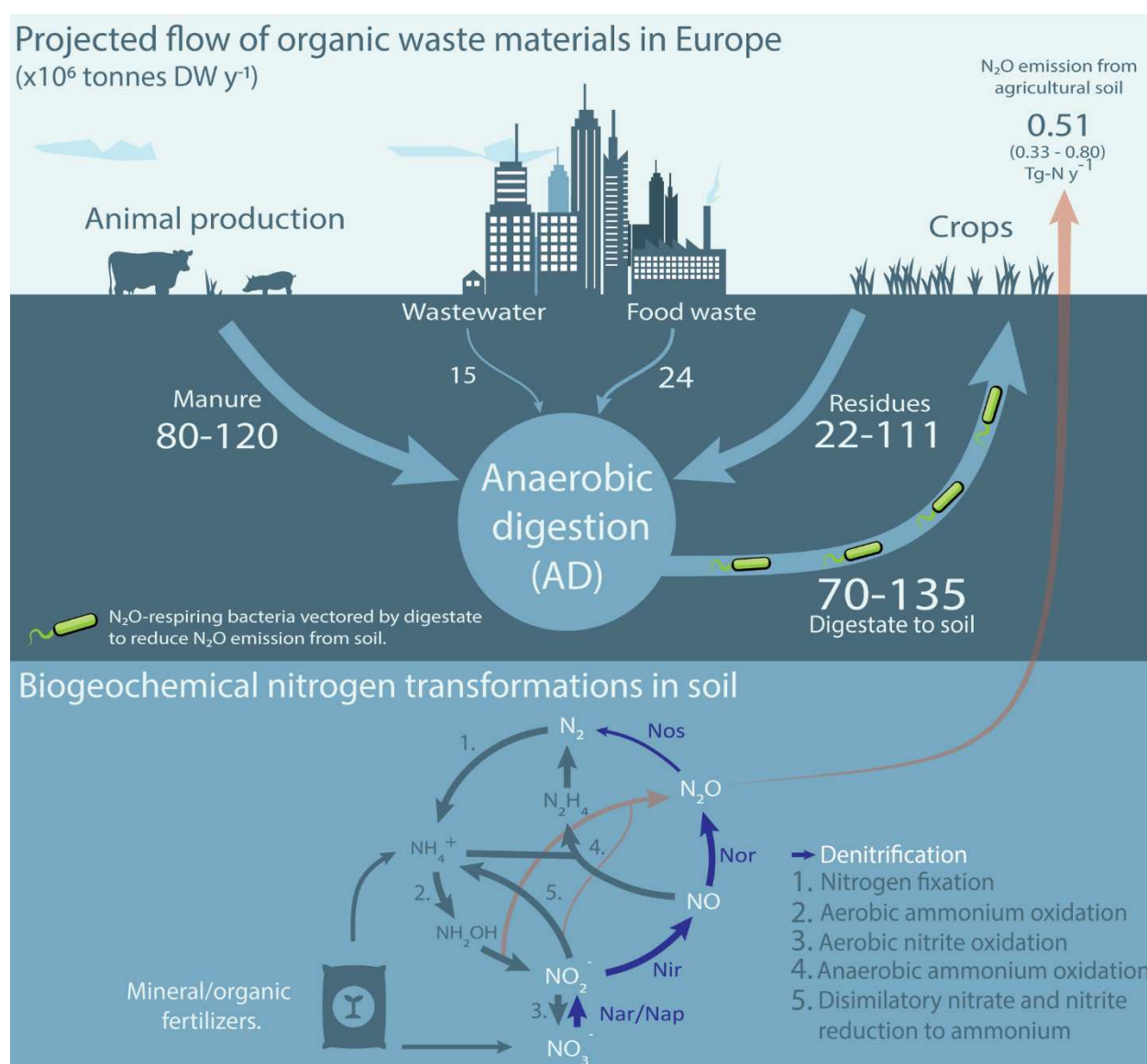
28 Nitrous oxide is an intermediate in the nitrogen cycle and a powerful greenhouse gas emitted  
29 in large volumes from agricultural soils, accounting for ~1/3 of total anthropogenic N<sub>2</sub>O  
30 emissions (Tian et al 2020). Reduced emissions can be achieved by minimizing the  
31 consumption of fertilizer nitrogen through improved agronomic practice and reduction of  
32 meat consumption (Snyder et al 2014, Sutton et al, 2011), but such measures are unlikely to  
33 do more than stabilize the global consumption of fertilizer N (Erisman et al 2008). This calls  
34 for more inventive approaches to reduce N<sub>2</sub>O emissions, targeting the microbiomes of soil  
35 (D'Hondt et al 2021), in particular the physiology and regulatory biology of the organisms  
36 involved in production and consumption of N<sub>2</sub>O in soil (Bakken and Frostegård 2020).

37 N<sub>2</sub>O turnover in soil involves several metabolic pathways, controlled by a plethora of  
38 fluctuating physical and chemical variables (Butterbach-Bahl et al 2013, Hu et al 2015).

39 Heterotrophic denitrification is the dominant N<sub>2</sub>O source in most soils, while autotrophic  
40 ammonia oxidation may dominate in well drained calcareous soils (Song et al 2018 and  
41 references therein). Heterotrophic denitrifying organisms are both sources and sinks for N<sub>2</sub>O  
42 because N<sub>2</sub>O is a free intermediate in their stepwise reduction of nitrate to dinitrogen (NO<sub>3</sub><sup>-</sup>  
43 →NO<sub>2</sub><sup>-</sup>→NO→N<sub>2</sub>O→N<sub>2</sub>). Denitrification involves four enzymes collectively referred to as  
44 denitrification reductases: nitrate reductase (Nar/Nap), nitrite reductase (Nir), nitric oxide  
45 reductase (Nor) and nitrous oxide reductase (Nos), encoded by the genes *nar/nap*, *nir*, *nor*  
46 and *nosZ*, respectively. Oxygen is a strong repressor of denitrification, both at the  
47 transcriptional and the metabolic level (Zumft 1997, Qu et al 2016). Many organisms have  
48 truncated denitrification pathways, lacking from one to three of the four reductase genes  
49 (Shapleigh 2013, Lycus et al 2017), and truncated denitrifiers can thus act as either N<sub>2</sub>O  
50 producers (organisms without *nosZ*) or N<sub>2</sub>O reducers (organisms with *nosZ* only). The  
51 organisms with *nosZ* only, coined non-denitrifying N<sub>2</sub>O-reducers (Sanford et al 2013), have  
52 attracted much interest as N<sub>2</sub>O sinks in the environment (Hallin et al 2018). Of note,  
53 organisms with a full-fledged denitrification pathway may also be strong N<sub>2</sub>O sinks depending  
54 on the relative activities and regulation of the various enzymes in the denitrification pathway  
55 (Lycus et al 2018; Mania et al 2020). Despite their promise, feasible ways to utilize N<sub>2</sub>O-  
56 reducing organisms to reduce N<sub>2</sub>O emissions have not yet emerged.

57 A soil with a strong N<sub>2</sub>O-reducing capacity will emit less N<sub>2</sub>O than one dominated by net N<sub>2</sub>O  
58 producing organisms, as experimentally verified by Domeignoz-Horta et al (2016), who  
59 showed that soils emitted less N<sub>2</sub>O if inoculated with large numbers (10<sup>7</sup> - 10<sup>8</sup> cells g<sup>-1</sup> soil) of  
60 organisms expressing Nos as their sole denitrification reductase. As a standalone operation,  
61 the large-scale production and distribution of N<sub>2</sub>O-respiring bacteria would be prohibitively  
62 expensive and impractical. However, the use of N<sub>2</sub>O-respiring bacteria could become feasible  
63 if adapted to an existing fertilization pipeline, such as fertilization with the nitrogen- and  
64 phosphate-rich organic waste (digestate) generated by biogas production in anaerobic  
65 digesters. Anaerobic digestion (**AD**) is already a core technology for treating urban organic  
66 wastes, and is expected to treat an increasing proportion of the much larger volumes of waste  
67 produced by the agricultural sector (**Figure 1**), as an element of the roadmap towards a low-  
68 carbon circular economy (Scarlat et al 2018). This means that digestates from **AD** are likely to  
69 become a major organic fertilizer for agricultural soils, with a huge potential for reducing N<sub>2</sub>O  
70 emissions if enriched with N<sub>2</sub>O-respiring bacteria prior to application.

71 Here we provide the first proof of this promising concept. Firstly, we demonstrate selective  
72 enrichment and isolation of fast-growing digestate-adapted N<sub>2</sub>O-respiring bacteria using a  
73 digestate from a wastewater treatment plant. Secondly, we demonstrate that the use of  
74 digestates enriched with such organisms as a soil amendment reduces the proportion of N  
75 leaving soil as N<sub>2</sub>O, confirming the suitability of such digestates for this purpose. Analysis of  
76 the enrichment process with multi-omics and in-depth monitoring of gas kinetics provides  
77 valuable insights into Nos-synthesis by the various enriched taxa, and the metabolic pathways  
78 of the anaerobic consortium providing substrates for these enriched N<sub>2</sub>O-respiring  
79 organisms.



80

81 **Figure 1. Possible biomass streams in a future circular economy with a central role for anaerobic digestion.**  
82 Solid arrows (top section) show streams of biomass available for anaerobic digestion (AD). Numbers indicate  
83 known estimates of currently used or potentially available amounts in Europe, in million tonnes dry-weight (DW)  
84 per year (Foged et al 2011, Holm-Nielsen et al 2009, Stenmarck et al 2016, Meyer et al 2018). The arrow from  
85 anaerobic digestion to agricultural soil, indicates a credible pathway for digestate enriched with  $N_2O$ -reducing  
86 bacteria (assuming enrichment at AD site); fertilization with such enriched digestates strengthens the  $N_2O$  sink  
87 capacity of the soil, hence reducing  $N_2O$  emissions.  $N_2O$  emissions from agricultural soil in Europe are estimated  
88 at 0.51 tG per year (min 0.33 – max 0.80), representing some 48 % of total European  $N_2O$  emissions (Tian et al  
89 2020), which account for approximately 3.5 % of the global warming effect from European greenhouse gas  
90 emissions and 35 % of the global warming effect from European agriculture (Eurostat 2018). The lower half of  
91 the picture shows the microbial nitrogen transformations underlying these  $N_2O$  emissions, which are fed by  
92 fertilizers. Today, AD is primarily used for treating urban organic wastes, which comprise only ~10 % of the  
93 biomass potentially available for AD. The amount of biomass treated by AD is expected to increase by an order  
94 of magnitude when adopted on a large scale in the agricultural sector. This would generate 70-135 Mt DW of  
95 digestate annually (assuming 50% degradation by AD), which is equivalent to 400-780 kg DW ha $^{-1}$  y $^{-1}$  if spread  
96 evenly on the total farmland of Europe (173 million ha).

97 **Materials and methods**

98 The digestates were taken from two anaerobic digesters, one mesophilic (37 °C) and one thermophilic  
99 (52 °C), which were running in parallel, producing biogas from sludge produced by a wastewater  
100 treatment. The sludge was a poly-aluminum chloride (PAX-XL61™, Kemira) and ferric chloride  
101 (PIX318™, Kemira) precipitated municipal wastewater sludge, with an organic matter content of 5.6%  
102 (w/w). Both digestors reduced the organic matter by approximately 60%, producing digestates  
103 containing ~2.1 % organic matter, 1.8-1.9 g NH<sub>4</sub><sup>+</sup>-N L<sup>-1</sup>, ~16 and 32 Meq VFA L<sup>-1</sup>, pH=7.6-7.8 and 8.2;  
104 mesophilic and thermophilic, respectively (see [Suppl Methods 1](#) for further details). The digestates  
105 were transported to the laboratory in 1 L insulated steel-vessels and used for incubation experiments  
106 3-6 hours after sampling.

107 The robotized incubation system developed by Molstad et al (2007, 2016) was used in all experiments  
108 where gas kinetics was monitored. The system hosts 30 parallel stirred batches in 120 mL serum vials,  
109 crimp sealed with gas tight butyl rubber septa, which are monitored for headspace concentration of  
110 O<sub>2</sub>, N<sub>2</sub>, N<sub>2</sub>O, NO, CO<sub>2</sub> and CH<sub>4</sub> by frequent sampling. After each sampling, the system returns an equal  
111 volume of He, and elaborated routines are used to account for the gas loss by sampling to calculate  
112 the production/consumption-rate of each gas for each time interval between two samplings. More  
113 details are given in [Suppl Methods 2](#).

114 Enrichment culturing of N<sub>2</sub>O-respiring bacteria (NRB) in digestate was done as stirred (300 rpm)  
115 batches of 50 mL digestate per vial. Prior to incubation, the headspace air was replaced with Helium  
116 by repeated evacuation and He-filling (Molstad et al 2007), and supplemented with N<sub>2</sub>O, and N<sub>2</sub>O in  
117 the headspace was sustained by repeated injections in response to depletion. Liquid samples (1 mL)  
118 were taken by syringe, for metagenomic and metaproteomic analyses, and for quantification of  
119 volatile fatty acids (VFA) and 16srDNA abundance. The samples were stored -80 °C before analyzed.  
120 The growth of NRB in the enrichments was modelled based on the N<sub>2</sub>O reduction kinetics. The  
121 modelling and the analytic methods (quantification of VFA and 16srDNA abundance) are described in  
122 detail in [Suppl Methods 3](#).

123 Metagenomics and metaprotomics: Sequencing of DNA (Illumina HiSec4000), and the methods for  
124 Metagenome-Assembled Genome (MAG) binning, and the phylogenetic placement of the MAGs is  
125 described in detail in [Suppl Methods 4](#). Proteins were extracted and digested to peptides, which were  
126 analyzed by nanoLC-MS/MS, and the acquired spectra were inspected, using the metagenome-  
127 assembled genomes (149 MAGs) as a scaffold ([Suppl Methods 5](#)).

128 Isolation of N<sub>2</sub>O-respiring bacteria (NRB) ([Suppl Methods 6](#)). NRB present in the enrichment cultures  
129 were isolated by spreading diluted samples on agar plates with different media composition, then  
130 incubated in an anaerobic atmosphere with N<sub>2</sub>O. Visible colonies were re-streaked and subsequently  
131 cultured under aerobic conditions, and 16s-sequenced. Three isolates, **AS** (*Azospira* sp), **AN** (*Azonexus*  
132 sp) and **SP** (*Pseudomonas* sp) (names based on their 16s sequence), were selected for genome  
133 sequencing, characterization of their denitrification phenotypes, and for testing their effect as N<sub>2</sub>O  
134 sinks in soil.

135 Genome sequencing and phenotyping of isolates. Three isolates were genome sequenced and  
136 compared with MAG's of the enrichment culture ([Suppl Methods 7](#)). The isolates' ability to utilize  
137 various organic C substrates was tested on BiOLOG Phenotype MicroArray™ microtiter plates, and  
138 their characteristic regulation of denitrification was tested through a range of incubation experiments  
139 as in previous investigations (Bergaust et al 2010, Liu et al 2014, Lycus et al 2018, Mania et al 2020),  
140 by monitoring the kinetics of O<sub>2</sub>, N<sub>2</sub>, N<sub>2</sub>O, NO and NO<sub>2</sub><sup>-</sup> throughout the cultures' depletion of O<sub>2</sub> and  
141 transition from aerobic to anaerobic respiration in stirred batch cultures with He + O<sub>2</sub> (+/- N<sub>2</sub>O) in the  
142 headspace ([Suppl Methods 8](#)). The kinetics of electron flow throughout the oxic and anoxic phase in

143 these experiments were used to assess if the organisms were *bet hedging*, as demonstrated for  
144 *Paracoccus denitrificans* (Lycus et al 2018), i.e. that only a minority of cells express nitrate- and/or  
145 nitrite-reductase, while all express Nos, in response to oxygen depletion. Putative *bet*  
146 *hedging* was corroborated by measuring the abundance of nitrate-, nitrite- and nitrous oxide  
147 reductase (Suppl Methods 9).

148 N<sub>2</sub>O mitigation experiments (Suppl Methods 9). To assess the capacity of the isolates to reduce the  
149 N<sub>2</sub>O emission from soil, they were grown aerobically in sterilized digestate, which was then added to  
150 soil in microcosms, for measuring the NO-, N<sub>2</sub>O- and N<sub>2</sub>- kinetics of denitrification in the soil. For  
151 comparison, the experiments included soils amended with sterilized digestate, live digestate (no  
152 pretreatment), and digestate in which N<sub>2</sub>O-reducing bacteria had been enriched by anaerobic  
153 incubation with N<sub>2</sub>O (as for the initial enrichment culturing).

154 *Data availability*

155 The sequencing data for this study have been deposited in the European Nucleotide Archive (ENA) at  
156 EMBL-EBI under accession number PRJEB41283 (isolates AN, AS and PS) and PRJEB41816  
157 (metagenome) (<https://www.ebi.ac.uk/ena/browser/view/PRJEBxxxx>). Functionally annotated MAGs  
158 and metagenomic assembly are available in FigShare (DOI: [10.6084/m9.figshare.13102451](https://doi.org/10.6084/m9.figshare.13102451) and  
159 [10.6084/m9.figshare.13102493](https://doi.org/10.6084/m9.figshare.13102493)). The proteomics data has been deposited to the ProteomeXchange  
160 Consortium (<http://proteomecentral.proteomexchange.org>) via the PRIDE partner repository  
161 (Vizcaino et al 2013) with the dataset identifier PXD022030\* and PXD023233\*\* for the metaproteome  
162 and proteome of *Azonexus* sp. AN, respectively.

163 \* Reviewer access: Username: [reviewer\\_pxd022030@ebi.ac.uk](mailto:reviewer_pxd022030@ebi.ac.uk). Password: GdTR3biE

164 \*\* Reviewers access: Username: [reviewer\\_pxd023233@ebi.ac.uk](mailto:reviewer_pxd023233@ebi.ac.uk) Password: nMz62S8O

165

166 **Results and Discussion**

167 Enrichment of indigenous N<sub>2</sub>O- respiration bacteria (NRB) in digestates

168 We hypothesized that suitable organisms could be found in anaerobic digesters fed with  
169 sewage sludge, since such sludge contains a diverse community of denitrifying bacteria  
170 stemming from prior nitrification/denitrification steps (Lu et al 2014). We further  
171 hypothesized that these bacteria could be selectively enriched in digestates by anaerobic  
172 incubation with N<sub>2</sub>O. We decided to enrich at 20 °C, rather than at the temperatures of the  
173 anaerobic digesters (37 and 52 °C), to avoid selecting for organisms unable to grow within the  
174 normal temperature range of soils.

175 The digestates were incubated anaerobically as stirred batch cultures with N<sub>2</sub>O in the  
176 headspace (He atmosphere), and the activity and apparent growth of N<sub>2</sub>O reducers was  
177 assessed by monitoring the N<sub>2</sub>O-reduction to N<sub>2</sub>. **Figure 2A** shows the results for the first  
178 experiment, where culture vials were liquid samples were taken at three time points (0, 115  
179 and 325 h) for metagenomics, metaproteomics, and quantification of 16S rDNA and volatile  
180 fatty acids (VFAs). N<sub>2</sub>O was periodically depleted (100-140 h) in this experiment, precluding  
181 detailed analysis of the growth kinetics throughout. This was avoided in the second  
182 enrichment, for which complete gas data are shown in **Figure 2BC**. Apart from the deviations  
183 caused by the temporary depletion of N<sub>2</sub>O in the first experiment, both experiments showed

184 very similar  $N_2$  production rates (**Figures 2B and S1B**). The gas kinetics of the second  
185 enrichment are discussed in detail below.

186 **Figure 2B** shows declining rates of  $N_2$ -production ( $V_{N_2}$ ) during the first 50 h, followed by  
187 exponential increase. This was modelled as the activity of two groups of NRB, one growing  
188 exponentially from low initial abundance, and one which was more abundant initially, but  
189 whose activity declined gradually (further explained in **Figure S1**). The modelling, indicated  
190 that the cell density of the growing NRB increased exponentially (specific growth rate,  $\mu = 0.1$   
191  $h^{-1}$ ) from a very low initial density ( $\sim 2.5 \cdot 10^3$  cells  $mL^{-1}$ ) to  $1.6 \cdot 10^8$  cells  $mL^{-1}$  after 110 h, and  
192 continued to increase at a gradually declining rate to reach  $\sim 3 \cdot 10^9$  cells  $mL^{-1}$  at the end of the  
193 incubation period (215 h). The modelled cell-specific electron flow rate ( $V_e$ , **Figure 2C**) was  
194 sustained at around 5 fmol  $e^-$  cell $^{-1}$   $h^{-1}$  during the exponential growth, and declined gradually  
195 thereafter, as the number of cells continued to increase, while the overall rate of  $N_2O$ -  
196 respiration remained more or less constant ( $V_{N_2}$ , **Figure 2B**). Enrichment culturing as shown  
197 in **Figure 2BC** was repeated three times, demonstrating that the characteristic  $N_2$  production  
198 kinetics was highly reproducible (**Figure S2**).

199 The provision of substrate for the  $N_2O$ -respiring bacteria can be understood by considering  
200 the enrichment culture as a continuation of the metabolism of the anaerobic digester (**AD**),  
201 albeit slowed down by the lower temperature (20 °C, versus 37 °C in the digester). In **AD**,  
202 organic polymers are degraded and converted to  $CO_2$  and  $CH_4$  through several steps,  
203 conducted by separate guilds of the methanogenic microbial consortium: 1) hydrolysis of  
204 polysaccharides to monomers by organisms with carbohydrate-active enzymes, 2) primary  
205 fermentation of the resulting monomers to volatile fatty acids (VFAs), 3) secondary  
206 fermentation of VFAs to acetate,  $H_2$  and  $CO_2$ , and 4) methane production from acetate,  $CO_2$ ,  
207  $H_2$ , and methylated compounds. By providing  $N_2O$  to this (anaerobic) system, organisms that  
208 respire  $N_2O$  can tap into the existing flow of carbon, competing with the methanogenic  
209 consortium for intermediates, such as monomeric sugars, VFAs (such as acetate) and  
210 hydrogen (Stams et al 2003). Thus, the respiration and growth of the  $N_2O$ -respiring bacteria  
211 is sustained by a flow of carbon for which the primary source is the depolymerization of  
212 organic polymers. It is possible that the retardation of growth after  $\sim 100$  h of enrichment was  
213 due to carbon becoming limiting. Thus, at this point, the population of  $N_2O$ -respiring  
214 organisms may have reached high enough cell densities to reap most of the intermediates  
215 produced by the consortium.

216 Parallel incubations of digestates without  $N_2O$  confirmed the presence of an active  
217 methanogenic consortium, sustaining a methane production rate of  $\sim 0.2$   $\mu\text{mol } CH_4 mL^{-1} h^{-1}$   
218 throughout (**Figure S3**). Methane production was inhibited by  $N_2O$ , and partly restored in  
219 periods when  $N_2O$  was depleted (**Figure 2A**, **Figures S3&S4**). We also conducted parallel  
220 incubations with  $O_2$  and  $NO_3^-$  as electron acceptors. These incubations showed that  
221 methanogenesis was completely inhibited by  $NO_3^-$ , and partly inhibited by  $O_2$  (concentration  
222 in the liquid ranged from 20 to 90  $\mu\text{M } O_2$ ) (**Figures S3**). The rates of  $O_2$  and  $NO_3^-$  reduction  
223 indicated that the digestate contained a much higher number of cells able to respire  $O_2$  and  
224  $NO_3^-$  than cells able to respire  $N_2O$  (**Figure S5A-C**). During the enrichment culturing with  $NO_3^-$   
225 , almost all reduced nitrogen appeared in the form of  $N_2O$  during the first 50 h (**Figure S5E**),

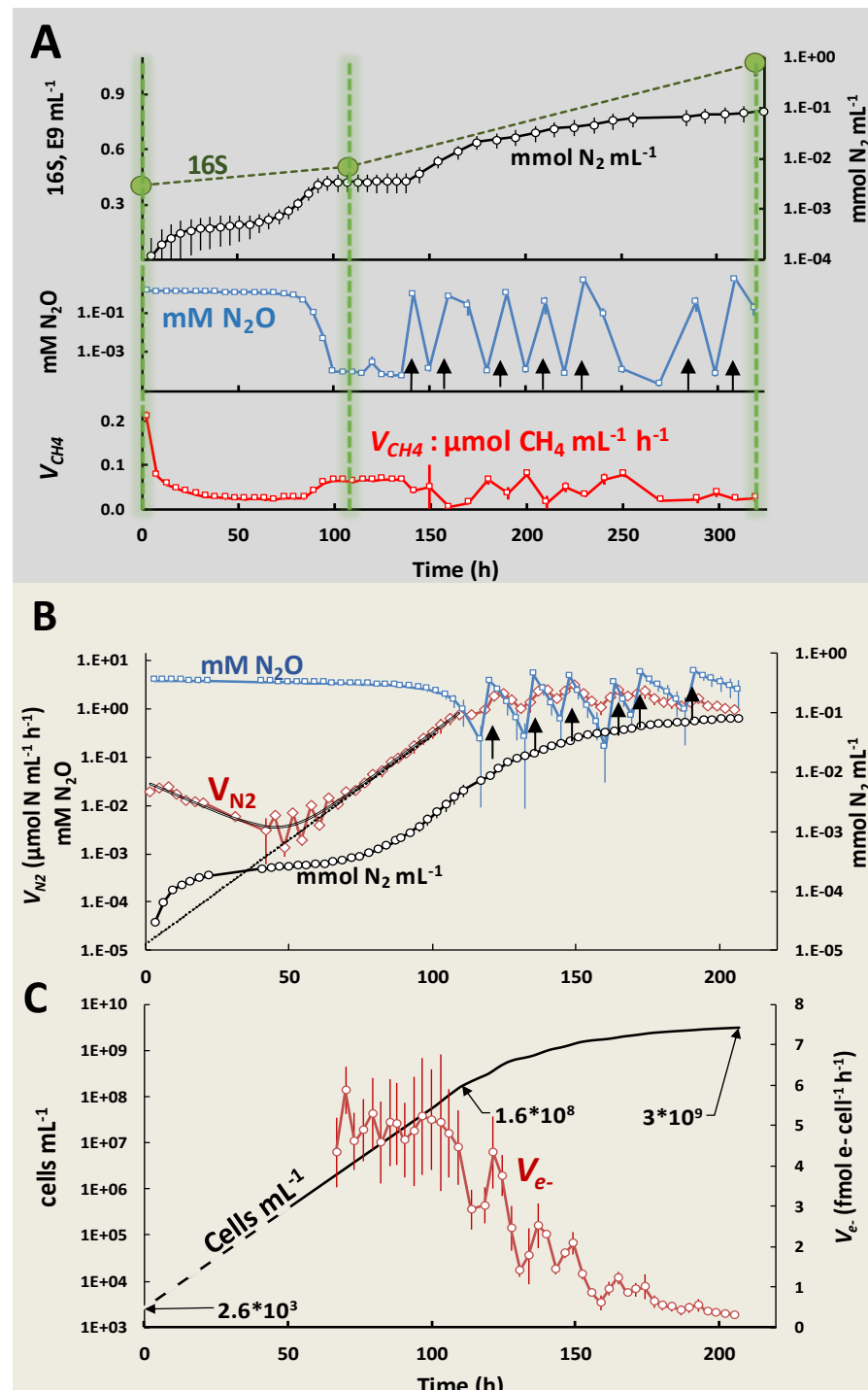
226 another piece of evidence that in the digestate (prior to enrichment culturing), the organisms  
227 reducing  $\text{NO}_3^-$  to  $\text{N}_2\text{O}$  outnumbered those able to reduce  $\text{N}_2\text{O}$  to  $\text{N}_2$ . The measured production  
228 of  $\text{CH}_4$  and electron flows to electron acceptors deduced from measured gases ( $\text{N}_2$ ,  $\text{O}_2$  and  
229  $\text{CO}_2$ ) were used to assess the effect of the three electron acceptors ( $\text{N}_2\text{O}$ ,  $\text{NO}_3^-$  and  $\text{O}_2$ ) on C-  
230 mineralization. While oxygen appeared to have a marginal effect,  $\text{NO}_3^-$  and  $\text{N}_2\text{O}$  caused severe  
231 retardation of C-mineralization during the first 50 and 100 h, respectively (**Figure S5A-D**). This  
232 retarded mineralization is plausibly due to the inhibition of methanogenesis, causing a  
233 transient accumulation of  $\text{H}_2$  and VFAs until the  $\text{N}_2\text{O}$ -reducing bacteria reach a cell density  
234 that allowed them to effectively reap these compounds. This was corroborated by  
235 measurements of  $\text{H}_2$  and VFAs (**Figure S13**).

236 To track the origin of the enriched  $\text{N}_2\text{O}$ -respiring bacteria in the digestate, we considered the  
237 possibility that these are indigenous wastewater-sludge bacteria that survive the passage  
238 through the anaerobic digester, which had a retention time of 20-24 days. We assessed  
239 survival of  $\text{N}_2\text{O}$ -respiring bacteria by comparing the  $\text{N}_2\text{O}$  reduction potential of wastewater  
240 sludge and the digestate. The results indicated that  $\leq 1/3$  of the  $\text{N}_2\text{O}$ -respiring bacteria in the  
241 sludge survived the passage (**Figure S6**). We also did enrichment culturing with a digestate  
242 from a thermophilic digester (52 °C) operated in parallel with the mesophilic digester  
243 (provided with the same feed), and found that it too contained  $\text{N}_2\text{O}$  reducers that could be  
244 enriched, although the estimated initial numbers were orders of magnitude lower than in the  
245 mesophilic digestate (**Figure S7**).

246 **Figure 2: Gas kinetics in**  
 247 **anaerobic enrichment**  
 248 **cultures with digestate.**

249 Panel A shows results for the  
 250 enrichment culture  
 251 (triplicate culture vials) sampled for metagenomics,  
 252 metaproteomics,  
 253 quantification of volatile  
 254 fatty acids (VFAs) and 16S  
 255 rDNA abundance (sampling  
 256 times = 0, 115 and 325 hours,  
 257 marked by vertical green  
 258 lines). The top panel shows  
 259 the amounts of  $N_2$  produced  
 260 (mmol  $N_2$  L<sup>-1</sup> digestate, log  
 261 scale) and 16S rDNA copy  
 262 numbers. The mid panel  
 263 shows the concentration of  
 264  $N_2O$  in the digestate (log  
 265 scale), which was  
 266 replenished by repeated  
 267 injections from  $t=140$  h and  
 268 onwards (indicated by black  
 269 arrows). The bottom panel  
 270 shows the rate of methane  
 271 production. Standard  
 272 deviations ( $n=3$ ) are shown  
 273 as vertical lines in all panels.

274 Panel B and C show the  
 275 results of a repeated  
 276 enrichment experiment  
 277 where  $N_2O$ -depletion (as  
 278 seen at  $t=100-140$  h in panel  
 279 A) was avoided, to allow  
 280 more precise assessment  
 281 and modelling of growth  
 282 kinetics. Panel B:  $N_2O$   
 283 concentration in the  
 284 digestate (mM  $N_2O$ ), rate of  
 285  $N_2$ -production ( $V_{N_2}$ ) and  $N_2$



286 produced (mmol  $N_2$  mL<sup>-1</sup> digestate), all log scaled. The curved black line shows the modelled  $V_{N_2}$  assuming two  
 287 populations, one growing exponentially ( $\mu = 0.1 \text{ h}^{-1}$ ), and one whose activity was dying out gradually (rate = -  
 288  $0.03 \text{ h}^{-1}$ ). The dotted black line is the activity of the exponentially growing population extrapolated to time=0.  
 289 Panel C shows the modelled density (cells mL<sup>-1</sup>) of cells growing by  $N_2O$  respiration, extrapolated back to  $t=0$  h  
 290 (dashed line), and the cell specific respiratory activity ( $V_e^-$ , fmol electrons cell<sup>-1</sup> h<sup>-1</sup>), which declined gradually  
 291 after 110 h. Standard deviations ( $n = 3$ ) are shown as vertical lines. **Figure S1** provides additional data for the  
 292 experiment depicted in Panel A, as well as a detailed description of the modelling procedures and their results.

294 **MAG-centric metaproteomic analysis of the enrichment cultures**

295 We analyzed the metagenome and metaproteome at three timepoints (0, 115 and 325 h,  
296 **Figure 2A**), to explore the effect of the anaerobic incubation with N<sub>2</sub>O on the entire microbial  
297 consortium, and to identify the organisms growing by N<sub>2</sub>O reduction. Metagenomic  
298 sequences were assembled and resultant contigs assigned to 278 metagenome-assembled  
299 genomes (MAGs), of which 149 were deemed to be of sufficient quality (completeness > 50%  
300 and contamination < 20%, Supplementary Data S1) for downstream analysis. The  
301 phylogenetic relationship and the relative abundance of the MAGs throughout the  
302 enrichment are summarized in **Figure 3**, which also shows selected features revealed by the  
303 combined metagenomic and metaproteomic analyses, including information about genes  
304 and detected proteins involved in N<sub>2</sub>O reduction, other denitrification steps, methanogenesis,  
305 syntrophic acetate oxidation and methane oxidation.

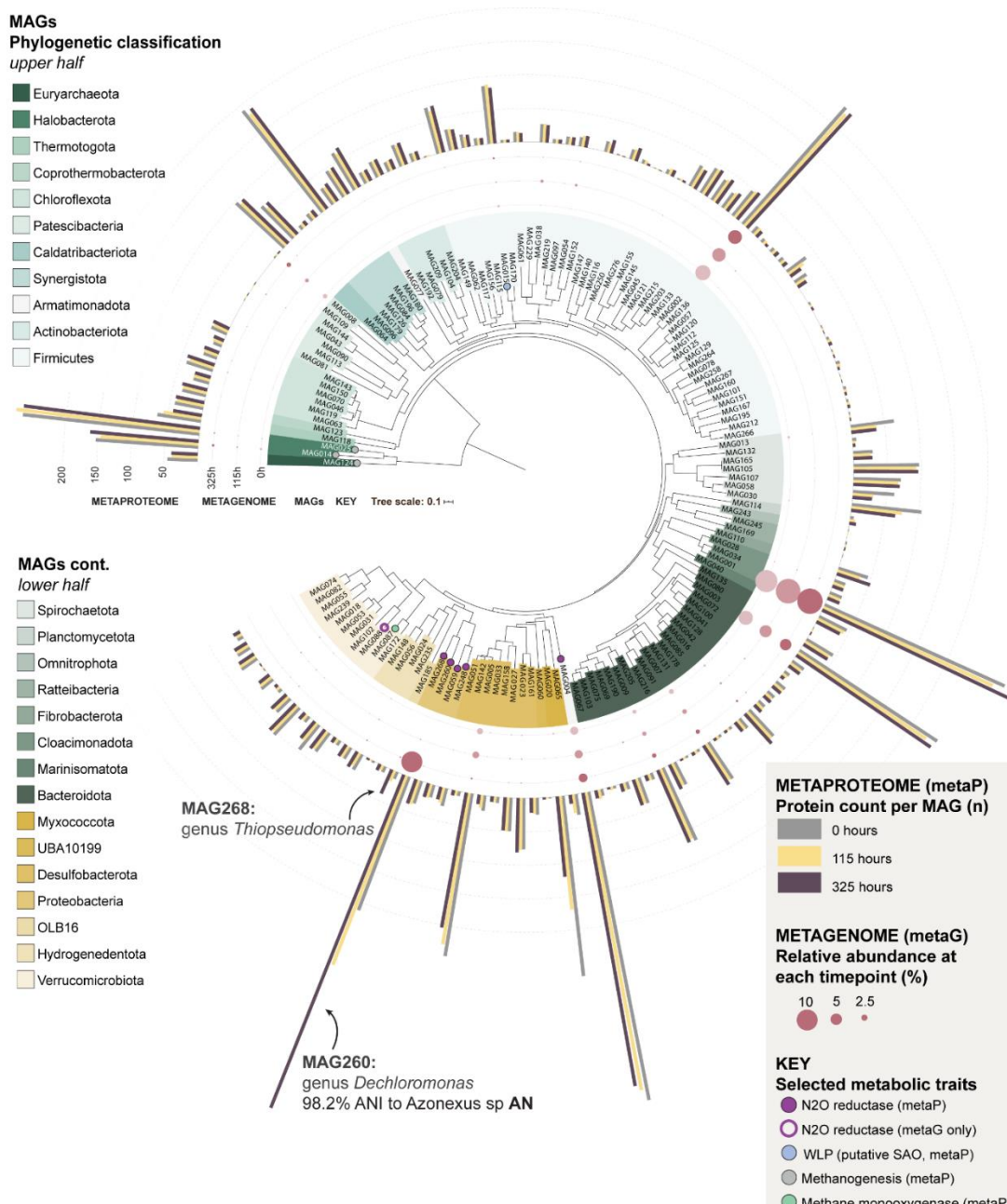
306 Closer inspections of the abundance of individual MAGs, based on their coverage in the  
307 metagenome and metaproteome, showed that the majority of the MAGs had a near constant  
308 population density throughout the incubation, while two MAGs (260 and 268) increased  
309 substantially (**Figure 4**; further analyses in **Supplementary Section B, Figures S8-S11**). The  
310 stable abundance of the majority indicates that the methanogenic consortium remained  
311 intact despite the downshift in temperature (20 °C versus 37 °C) and the inhibition of  
312 methanogenesis by N<sub>2</sub>O. Only 9 MAGs showed a consistent decline in abundance throughout  
313 the enrichment (**Table S1**). These MAGs could theoretically correspond to microbes whose  
314 metabolism is dependent on efficient H<sub>2</sub> scavenging by methanogens (Schink 1997), but we  
315 found no genomic evidence for this, and surmise that organisms circumscribed by the  
316 declining MAGs were unable to adapt to the temperature downshift from 37 °C to 20 °C.

317 Six MAGs, including the two that were clearly growing (MAG260 & MAG268) contained the  
318 *nosZ* gene and thus had the genetic potential to produce N<sub>2</sub>O-reductase (Nos) (**Figure 4**). Nos  
319 proteins originating from five of these MAGs were detected in the metaproteome.  
320 Importantly, while all but one of these MAGs contained genes encoding the other  
321 denitrification reductases, none of these were detected in the metaproteome, suggesting  
322 that the organisms can regulate the expression of their denitrification machinery to suit  
323 available electron acceptors, in this case N<sub>2</sub>O. Three of the MAGs with detectable Nos in the  
324 proteome (MAG004, MAG059, MAG248) appeared to be non-growing during the enrichment.  
325 The detected levels of their Nos proteins remained more or less constant, and their estimated  
326 abundance in the metagenome and -proteome did not increase (**Figure 4B**). It is conceivable  
327 that these three MAGs belong to the initial population of N<sub>2</sub>O reducers whose N<sub>2</sub>O-reduction  
328 activity was present initially but gradually decreased during the early phase of the enrichment  
329 (**Figure 2A**). The two growing MAGs (MAG260 and MAG268) showed increasing Nos levels  
330 and increasing abundance both in terms of coverage and metaproteomic detection (**Figure**  
331 **4B**), in proportion with the N<sub>2</sub> produced (**Figure S11**). MAG260 reached the highest  
332 abundance of the two and accounted for 92% of the total detectable Nos pool at the final  
333 time point. MAG260 is taxonomically most closely affiliated with the genus *Dechloromonas*  
334 (GTDB, 97.9% amino acid similarity). Interestingly, Nap rather than Nar takes the role of  
335 nitrate reductase in MAG260 (**Figure 4**), which makes it a promising organism for N<sub>2</sub>O  
336 mitigation since organisms with Nap only (lacking Nar) preferentially channel electrons to N<sub>2</sub>O  
337 rather than to NO<sub>3</sub><sup>-</sup> (Mania et al 2020). MAG260, MAG004 and MAG088 contain a clade II

338 *nosZ*, characterized by a *sec*-dependent signal peptide, in contrast to the more common *tat*-  
339 dependent clade I *nosZ*. The physiological implications of clade I versus clade II *nosZ* remains  
340 unclear. Organisms with *nosZ* Clade II have high growth yield and high affinity (low  $k_s$ ) for N<sub>2</sub>O,  
341 compared to those with *nosZ* Clade II (Yoon et al 2016), suggesting a key role of *nosZ* Clade II  
342 organisms for N<sub>2</sub>O reduction in soil, but this was contested by Conthe et al (2018), who found  
343 that Clade I organisms had higher “catalytic efficiency” ( $V_{max}/k_s$ ) than those with Clade II.

344 The apparent inhibition of methanogenesis by N<sub>2</sub>O seen in the present study has been  
345 observed frequently (Andalib et al 2011) and is probably due to inhibition of coenzyme M  
346 methyltransferase (Kengen et al 1988), which is a membrane bound enzyme essential for  
347 methanogenesis and common to all methanogenic archaea (Fischer et al 1992). The gas  
348 kinetics demonstrate that the inhibition of was reversible, being partly restored whenever  
349 N<sub>2</sub>O was depleted (**Figure 2**). In the enrichment culture where metagenomics and  
350 metaproteomics was monitored, several such incidents of N<sub>2</sub>O depletion occurred (**Figure 2A**)  
351 and during these periods CH<sub>4</sub> accumulated to levels amounting to 10% of levels in control  
352 vials without N<sub>2</sub>O (**Figure S4B**). These observations suggest that methanogens would be able  
353 to grow, albeit sporadically, during the enrichment, which is corroborated by the sustained  
354 detection of the complete methanogenesis pathway, including the crucial coenzyme M  
355 methyl-transferase, of *Methanothrix* (MAG025), *Methanoregulaceae* (MAG014) and  
356 *Methanobacterium* (MAG124) at high levels in the metaproteome. In fact, both MAG  
357 coverage data and 16S rDNA copy numbers assessed by ddPCR suggested that the majority of  
358 the original methanogenic consortium continued to grow (**Supplementary Section B**). A  
359 tentative map of the metabolic flow of the methanogenic consortium, including the reaping  
360 of intermediates (monosaccharides, fatty acids, acetate and H<sub>2</sub>) by N<sub>2</sub>O-respiring bacteria is  
361 shown in **Figure S12**. Since methane production was inhibited from the very beginning of the  
362 incubation, while it took ~100 hours for the N<sub>2</sub>O-respiring bacteria to reach high enough  
363 numbers to become a significant sink for intermediates (**Figure 2**), one would expect transient  
364 accumulation of volatile fatty acids and H<sub>2</sub>, which was corroborated by measurements of  
365 these metabolites (**Figure S13**).

366 Of note, we detected methane monooxygenase and methanol dehydrogenase proteins from  
367 MAG087 and MAG059, respectively, in the metaproteome. This opens up the tantalizing  
368 hypothesis of N<sub>2</sub>O-driven methane oxidation, a process only recently suggested to occur  
369 (Valenzuela et al 2020; Cheng et al 2019). However, a close inspection of the N<sub>2</sub>O- and CH<sub>4</sub>-  
370 kinetics indicated that N<sub>2</sub>O-driven methane oxidation played a minor role (**Figure S4CD**).



394 **Figure 3: MAGs from the anaerobic enrichment culture with the mesophilic digestate.** The figure shows a  
395 maximum likelihood tree indicating the phylogenetic placement of MAGs from the anaerobic enrichment. The  
396 tree was constructed from a concatenated set of protein sequences of single-copy genes. Taxonomic  
397 classification of the MAGs was inferred using the Genome Taxonomy Database (GTDB) and is displayed at the  
398 phylum level by label and branch coloring. Branch label decorations indicate the presence of genes involved in  
399 selected metabolic traits in the MAGs. The relative abundance of the MAG in the community as calculated from  
400 sequence coverage is indicated by bubbles at branch tips and bar charts indicate the number of detected  
401 proteins affiliated with each MAG at the three time points during incubation. Four of the 149 MAGs that met  
402 the completeness and contamination threshold for construction of the metaproteome database were lacking  
403 the universal single-copy marker genes and were omitted from the tree. Total protein counts per MAG were  
404 calculated by aggregating both secretome and cell-associated proteomes.

405 Isolation of N<sub>2</sub>O-respiring bacteria and their geno- and phenotyping

406 Whilst this enrichment culture could be used directly as a soil amendment, this approach is  
407 likely to have several disadvantages. First, it would require the use of large volumes of N<sub>2</sub>O

408 for enrichment, a process which would be costly and require significant infrastructure. An  
409 alternative approach would be to introduce an axenic or mixed culture of digestate-derived,  
410 and likely digestate-adapted, N<sub>2</sub>O-respiring bacteria to sterilized/sanitized digestates. This  
411 approach has multiple benefits: 1) it would remove the need for N<sub>2</sub>O enrichment on site as  
412 isolates could be grown aerobically in the digestate material, 2) one could chose organisms  
413 with favorable denitrification genotypes and regulatory phenotypes, 3) the sanitation would  
414 eliminate the methanogenic consortium hence reducing the risk of methane emissions from  
415 anoxic micro-niches in the amended soil, and 4) sanitation of digestates aligns with current  
416 practices that require such a pretreatment prior to use for fertilization. For these reasons an  
417 isolation effort was undertaken to obtain suitable digestate-adapted N<sub>2</sub>O-respiring  
418 microorganisms from the N<sub>2</sub>O-enrichment cultures. These efforts resulted in the recovery of  
419 three axenic N<sub>2</sub>O-respiring bacterial cultures, which were subjected to subsequent genomic  
420 and phenotypic characterization.

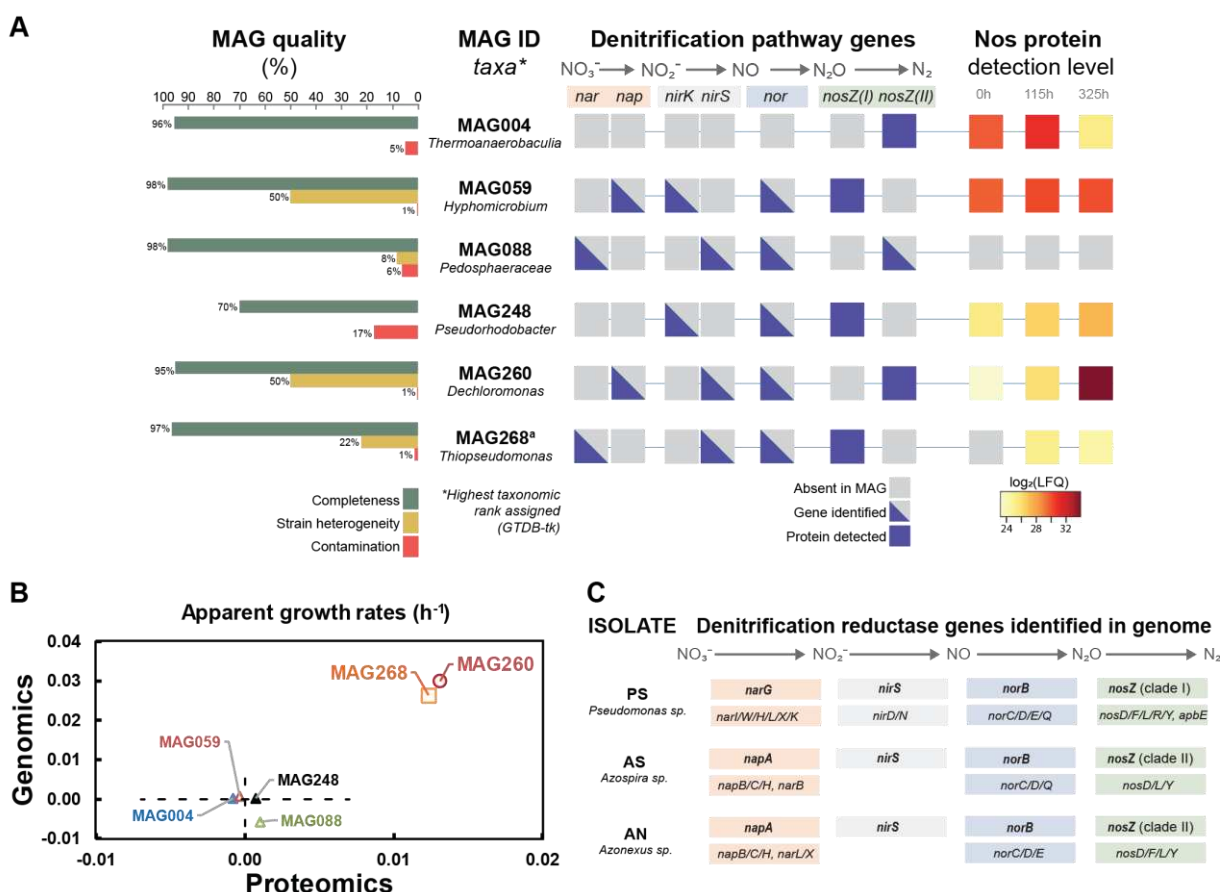
421 The isolates were phylogenetically assigned to *Pseudomonas* sp. (**PS**), *Azospira* sp. (**AS**) and  
422 *Azonexus* sp. (**AN**) (working names in bold) based on full length 16S rDNA obtained from the  
423 sequenced genomes (accessions ERR4842639 - 40, **Table S2**, phylogenetic trees shown in  
424 **Figure S14**). All were equipped with genes for a complete denitrification pathway (**Figure 4C**).  
425 **AN** and **AS** carried *napAB*, encoding the periplasmic nitrate reductase (Nap) and *nosZ* clade II,  
426 whilst **PS** carried genes for the membrane bound nitrate reductase (Nar), encoded by *narG*,  
427 and *nosZ* clade I. All had *nirS* and *norBC*, coding for nitrite reductase (NirS) and nitric oxide  
428 reductase (Nor), respectively. Pairwise comparison of average nucleotide identities (ANI) with  
429 MAGs from the enrichment metagenomes showed that the isolate **AN** matched the  
430 *Dechloromonas*-affiliated MAG260 with 98.2 % ANI, suggesting the isolate is circumscribed by  
431 MAG260 (Richter and Resselló-Móra 2009). Given the GTDB phylogeny of **AN** and MAG260  
432 and the 16S rDNA gene homology of **AN** (95.2 % sequence identity to *Azonexus hydrophilus*  
433 DSM23864, **Fig S14C**), we conclude that **AN** likely represents a novel species within the  
434 *Azonexus* lineage. Unfortunately, the 16S rDNA gene was not recovered in MAG260,  
435 preventing direct comparison with related populations. No significant ANI matches in our  
436 MAG inventory were identified for the genomes of **PS** and **AS**.

437 The carbon catabolism profiles of the isolates were assayed using Biolog<sup>TM</sup> PM1 and PM2  
438 microplates, to screen the range of carbon sources utilized (**Supplementary Section E**). **PS**  
439 utilized a wide spectrum of carbon sources (amino acids, nucleic acids, volatile fatty acids  
440 (VFA), alcohols, sugar alcohols, monosaccharides and amino sugars), but only one polymer  
441 (laminarin). **AN** and **AS** could only utilize small VFAs (eg. acetate, butyrate), intermediates in  
442 the TCA cycle and/or the β-oxidation/methyl malonyl-CoA pathways of fatty acid degradation  
443 (eg. malate, fumarate, succinate), and a single amino acid (glutamate). Thus, all three would  
444 be able to grow in a live digestate by reaping the VFA's produced by the methanogenic  
445 consortium. While the utilization of VFAs as C-substrates is one of several options for **PS**, **AN**  
446 and **AS** appear to depend on the provision of VFAs. This was confirmed by attempts to grow  
447 the three isolates in an autoclaved digestate: while **PS** grew well and reached high cell  
448 densities without any provision of extra carbon sources, **AN** and **AS** showed early retardation  
449 of growth unless provided with an extra dose of suitable carbon source (glutamate, acetate,  
450 pyruvate or ethanol) (**Figure S25 and S26**). A high degree of specialization and metabolic

451 streamlining may thus explain the observed dominance of **AN** (MAG260) during enrichment  
452 culturing.

453 To evaluate the potentials of these isolates to act as sinks for N<sub>2</sub>O, we characterized their  
454 denitrification phenotypes, by monitoring kinetics of oxygen depletion, subsequent  
455 denitrification and transient accumulation of denitrification intermediates (NO<sub>2</sub><sup>-</sup>, NO, N<sub>2</sub>O).  
456 The experiments were designed to assess properties associated with strong N<sub>2</sub>O reduction  
457 such as 1) *bet hedging*, i.e. that all cells express N<sub>2</sub>O reductase while only a fraction of the  
458 cells express nitrite- and/or nitrate-reductase, as demonstrated for *Paracoccus denitrificans*  
459 (Lycus et al 2018); 2) strong metabolic preference for N<sub>2</sub>O-reduction over NO<sub>3</sub><sup>-</sup>-reduction, as  
460 demonstrated for organisms with periplasmic nitrate reductase (Mania et al 2020).  
461 **Supplementary section F** provides the results of all the experiments and a synopsis of the  
462 findings. In short: *Azonexus* sp. (**AN**) had a clear preference for N<sub>2</sub>O over NO<sub>3</sub><sup>-</sup> reduction, but  
463 not over NO<sub>2</sub><sup>-</sup> reduction, ascribed to *bet hedging* with respect to the expression of nitrate  
464 reductase (a few cells express Nap, while all cells express Nos), which was corroborated by  
465 proteomics: the Nos/Nap abundance ratio was ~25 during the initial phase of denitrification  
466 (**Figure S17**). *Azospira* sp. (**AS**) had a similar preference for N<sub>2</sub>O over NO<sub>3</sub> reduction, albeit less  
467 pronounced than in **AN**, and no preference for N<sub>2</sub>O over NO<sub>2</sub><sup>-</sup>. *Pseudomonas* sp. (**PS**) showed  
468 a phenotype resembling that of *Paracoccus denitrificans* (Lycus et al 2018), with  
469 denitrification kinetics indicating that Nir is expressed in a minority of cells in response to O<sub>2</sub>  
470 depletion, while all cells appeared to express N<sub>2</sub>O reductase. This regulation makes **PS** a more  
471 robust sink for N<sub>2</sub>O than the two other isolates, since it kept N<sub>2</sub>O extremely low even when  
472 provided with NO<sub>2</sub><sup>-</sup>.

473 In summary, **PS** appeared to be the most robust candidate as a sink for N<sub>2</sub>O in soil for two  
474 reasons; 1) it can utilize a wide range of carbon substrates, and 2) its N<sub>2</sub>O sink strength is  
475 independent of the type of nitrogen oxyanion present (NO<sub>2</sub><sup>-</sup> or NO<sub>3</sub><sup>-</sup>). In contrast, **AN** and **AS**  
476 appear to be streamlined for harvesting intermediates produced by anaerobic consortia,  
477 hence their metabolic activity in soil could be limited. In addition, they could be sources rather  
478 than sinks for N<sub>2</sub>O if provided with NO<sub>2</sub><sup>-</sup>, which is likely to happen in soils, at least in soils of  
479 neutral pH, during hypoxic/anoxic spells (Lim et al 2018).



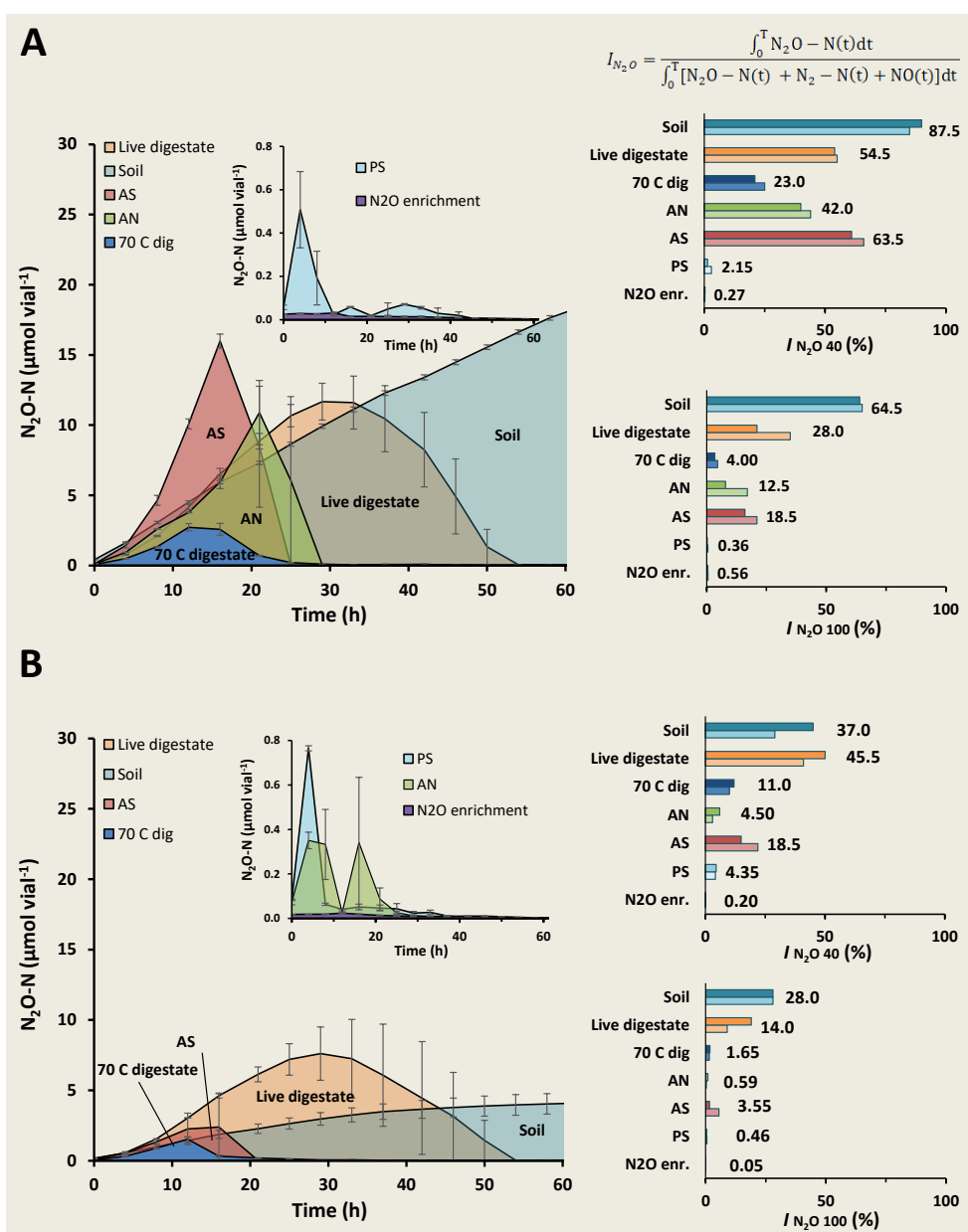
504 digestate (directly from the digester), and live digestate heated to 70 °C for 2 hours (to  
505 eliminate most of the indigenous consortium). In all cases, 3 mL of digestate was added to 10  
506 g of soil. Since soil acidity has a pervasive effect on the synthesis of functional N<sub>2</sub>O reductase  
507 (Liu et al 2014), we tested the digestates with two soils from a liming experiment (Nadeem et  
508 al 2020) with different pH (pH<sub>CaCl<sub>2</sub></sub> = 5.5 and 6.6).

509 The transient N<sub>2</sub>O accumulation during denitrification was generally higher in the acid than in  
510 the near-neutral soil (**Figure 5**), which was expected since the synthesis of functional Nos is  
511 hampered by low pH (Bergaust et al 2010, Liu et al 2014). Based on the kinetics of both N<sub>2</sub>  
512 and N<sub>2</sub>O (see **Figure S27 and S28**), we calculated the N<sub>2</sub>O-index (*I<sub>N2O</sub>*) which is a measure of  
513 the molar amounts of N<sub>2</sub>O relative to N<sub>2</sub>+N<sub>2</sub>O in the headspace for a specific period (0-T), see  
514 equation at top of **Figure 5**). Low values of *I<sub>N2O</sub>* indicate efficient N<sub>2</sub>O-reduction. In this case,  
515 we calculated *I<sub>N2O</sub>* for the incubation period until 40% of the available NO<sub>3</sub><sup>-</sup> had been  
516 recovered as N<sub>2</sub>+N<sub>2</sub>O (=*I<sub>N2O</sub> 40*) and for the incubation period until 100% was recovered (*I<sub>N2O</sub> 100*).  
517

518 Extremely low *I<sub>N2O</sub>* values were recorded for the treatments with digestate in which N<sub>2</sub>O-  
519 reducing bacteria were enriched by anaerobic incubation with N<sub>2</sub>O, even in the acid soil. This  
520 is in line with the current understanding of how pH affects N<sub>2</sub>O-reduction: low pH slows down  
521 the synthesis of functional Nos, but once synthesized, it remains functional even at low pH  
522 (Bergaust et al 2010). Functional Nos had already been expressed during the enrichment and  
523 was evidently active after amendment to the soils.

524 *I<sub>N2O</sub>* values were generally high for treatment with live digestate, which probably reflects that  
525 the digestate is dominated by N<sub>2</sub>O-producing organisms (**Figure S5E**). This interpretation is  
526 corroborated by the observed effect of heat-treating the live digestate; this lowered *I<sub>N2O</sub>*  
527 substantially.

528 The presence of the isolates in the digestates had clear but variable effects on *I<sub>N2O</sub>*. Compared  
529 to the heat treated digestate (“70 C dig” Fig 5), **AN** and **AS** increased the *I<sub>N2O</sub>*-values in the  
530 soil with pH=5.5, while in the soil with pH 6.6, their effect was marginal. The high *I<sub>N2O</sub>* for **AN**  
531 and **AS** in the acid soil plausibly reflect that the isolates were grown aerobically in the  
532 digestate, hence synthesizing their denitrification enzymes after transfer to soil, which would  
533 be hampered by low pH. In contrast to **AN** and **AS**, **PS** resulted in very low *I<sub>N2O</sub>* values in both  
534 soils, suggesting that this organism has an exceptional capacity to synthesize functional Nos  
535 at low pH.



536

537 **Figure 5: Soil incubations.**  $N_2O$  kinetics during incubation of soils amended with six different digestates and a  
 538 control sample (soil only). Panel A shows results for the pH 5.5 soil, while panel B the pH 6.6 soil. The digestates  
 539 treatments are: "Live digestate", digestate directly from the anaerobic digester; "70 C dig", live digestate heat  
 540 treated to 70 °C for two hours; AN, AS and PS: autoclaved digestate on which isolates AN, AS and PS had been  
 541 grown aerobically (see Figure S25&S26 for details on the cultivation); "N<sub>2</sub>O enr"= digestate enriched with N<sub>2</sub>O-  
 542 respiring bacteria (as in Fig 2). The left panels show the N<sub>2</sub>O levels observed during each treatment; the insets,  
 543 with altered scaling, show N<sub>2</sub>O levels for treatments that resulted in very low N<sub>2</sub>O levels (the PS and N<sub>2</sub>O enr.  
 544 treatments). The bar graphs to the right show the N<sub>2</sub>O indexes ( $I_{N_2O}$ , bar height = single culture vial values,  
 545 numerical value = average of duplicate culture vials), which are calculated by dividing the area under the N<sub>2</sub>O-  
 546 curve by the sum of the areas under the N<sub>2</sub>O and N<sub>2</sub>-curve, expressed as % (see equation in the figure and Liu et  
 547 al 2014; the N<sub>2</sub> curves are provided in Figures S27&S28).  $I_{N_2O}$  have proven to be a robust proxy for potential N<sub>2</sub>O  
 548 emission from soil (Russeñes et al 2016). Two  $I_{N_2O}$  values are shown: one for the timespan until 40% of the NO<sub>3</sub><sup>-</sup>  
 549 -N was recovered as N<sub>2</sub>+N<sub>2</sub>O+NO ( $I_{N_2O} 40\%$ ), and one for 100% recovery ( $I_{N_2O} 100\%$ ). More details (including N<sub>2</sub> and  
 550 NO kinetics) are shown in Figure S27 and S28.

551 These results show that the emission of N<sub>2</sub>O from soil fertilized with digestates can be  
 552 manipulated by tailoring the digestate microbiome. Interestingly, measurements of methane

553 in these soil incubations showed that the methanogenic consortia in digestates that had not  
554 been heat treated (i.e. the live digestate and the N<sub>2</sub>O enrichment) remained metabolically  
555 intact in the soil, and started producing methane as soon as N<sub>2</sub>O and nitrogen oxyanions had  
556 been depleted, while no methane was produced in the soils amended with autoclaved  
557 digestate, and that heated to 70 °C (**Figure S29**).

558 In an effort to determine the survival of the N<sub>2</sub>O-scavenging capacity of a digestate enriched  
559 with N<sub>2</sub>O reducers, we also tested its effect on soil N<sub>2</sub>O emissions after a 70-hour aerobic  
560 storage period (in soil or as enrichment culture, at 20 °C). These experiments demonstrated  
561 a sustained beneficial effect on  $I_{N2O}$  after 70 hours of aerobic storage (**Figure S30**). This result  
562 indicates that the enrichment strategies discussed here are robust, although long-lasting  
563 storage experiments as well as field trials are needed.

564 **Concluding remarks**

565 This feasibility study identifies an avenue for large scale cultivation of N<sub>2</sub>O reducers for soil  
566 application, which could be low cost if implemented as an add-on to biogas production  
567 systems. Further efforts should be directed towards selecting organisms that are both strong  
568 sinks for N<sub>2</sub>O and able to survive and compete in soil, to secure long-lasting effects on N<sub>2</sub>O  
569 emissions. A tantalizing added value would be provided by selecting organisms (or consortia  
570 of organisms) that are not only strong N<sub>2</sub>O-sinks, but also promote plant growth and disease  
571 resistance (Gao et al 2016, 2017).

572 Gas kinetics, metagenomics and metaproteomics revealed that the methanogenic consortium  
573 of the digestate remains active during anaerobic incubation with N<sub>2</sub>O, and that bacteria with  
574 an anaerobic respiratory metabolism grew by harvesting fermentation intermediates. The  
575 inhibition of methanogenesis by N<sub>2</sub>O implies that the respiring organisms would have  
576 immediate access to the electron donors that would otherwise be used by the methanogens,  
577 i.e. acetate and H<sub>2</sub>, while they would have to compete with fermentative organisms for the  
578 “earlier” intermediates such as alcohols and VFA. The importance of fermentation  
579 intermediates as a carbon source for the N<sub>2</sub>O-respiring bacteria would predict a selective  
580 advantage for organisms with a streamlined (narrow) catabolic capacity, i.e. limited to short  
581 fatty acids, and our results lend some support to this: the catabolic capacity of the organism  
582 that became dominant (MAG260, isolate **AN**) was indeed limited, as was also the case for  
583 isolate **AS**. Such organisms are probably not ideal N<sub>2</sub>O-sinks in soil because their ability to  
584 survive in this environment would be limited. Organisms with a wider catabolic capacity, such  
585 as the isolated *Pseudomonas* sp. (**PS**), are stronger candidates for long term survival and N<sub>2</sub>O-  
586 reducing activity in soil. The ideal organisms are probably yet to be found, however, and  
587 refinements of the enrichment culturing process are clearly needed.

588 The digestate used in this study contained N<sub>2</sub>O-respiring bacteria, most likely survivors from  
589 the raw sludge, which however, were clearly outnumbered by bacteria that are net producers  
590 of N<sub>2</sub>O. We surmise that the relative amounts of N<sub>2</sub>O-producers and N<sub>2</sub>O-reducers in  
591 digestates may vary, depending on the feeding material and configuration for the anaerobic  
592 digestion. This could explain the observed large variation of digestates on N<sub>2</sub>O emission from  
593 soils (Baral et al 2017, Herrero et al 2016). The high abundance of both NO<sub>3</sub><sup>-</sup> - and O<sub>2</sub>-respiring

594 organisms in digestates has practical implications for the attempts to grow isolated strains in  
595 digestates: they could be outnumbered by the indigenous  $\text{NO}_3^-$  - and  $\text{O}_2$ -respiring organisms  
596 (**Figure S5**). Hence, we foresee that future implementation of this strategy will require a brief  
597 heat treatment or other sanitizing procedure. A bonus of such sanitation is that it eliminates  
598 methane production by the digestate in soil.

599 We failed to enrich organisms lacking all other denitrification genes than *nosZ*; the only  
600 reconstructed genome with *nosZ* only (**MAG004**) did not grow at all. Failure to selectively  
601 enrich such organisms by anaerobic incubation with  $\text{N}_2\text{O}$  was also experienced by Conthe et  
602 al (2018). The organisms that did grow by respiring  $\text{N}_2\text{O}$  in our enrichment, were all equipped  
603 with genes for the full denitrification pathway, although the only denitrification enzyme  
604 expressed/detected during the enrichment was Nos. This agrees with the current  
605 understanding of the gene regulatory network of denitrification; *nosZ* is the only gene whose  
606 transcription does not depend on the presence of  $\text{NO}_3^-$ ,  $\text{NO}_2^-$  or  $\text{NO}$  (Spiro 2016), which were  
607 all absent during the enrichment.

608 Two of the reconstructed MAGs had periplasmic nitrate reductase (*nap*), as was the case for  
609 two of the three isolates (AN and AS). This in itself would predict preference for  $\text{N}_2\text{O}$ - over  
610  $\text{NO}_3^-$  reduction at a metabolic level (Mania et al 2020), but otherwise their potential for being  
611  $\text{N}_2\text{O}$  sinks cannot be predicted by their genomes. The phenotyping of the isolates revealed  
612 conspicuous patterns of *bet hedging* as demonstrated for *Paracoccus denitrificans* (Lycus et al  
613 2018). The *bet hedging* in *P. denitrificans* is characterized by expression of Nir (and Nor) in a  
614 minority of the cells, while Nos is expressed in all cells, in response to oxygen depletion, hence  
615 the population as a whole is a strong sink for  $\text{N}_2\text{O}$ . The isolated *Pseudomonas* sp. (PS)  
616 displayed denitrification kinetics that closely resembles that of *P. denitrificans*. The two other  
617 isolates (**AN** and **AS**) showed indications of *bet hedging* as well, but of another sort: Nap  
618 appears to be expressed in a minority of the cells. This different regulatory phenotype had  
619 clear implications for the ability of organisms to function as  $\text{N}_2\text{O}$ -sinks: while all isolates were  
620 strong  $\text{N}_2\text{O}$  sinks when provided with  $\text{NO}_3^-$  only, **AN** and **AS** accumulated large amounts of  
621  $\text{N}_2\text{O}$  if provided with  $\text{NO}_2^-$ .

622 The  $\text{N}_2\text{O}$  sink capacity of the organisms was tested by fertilizing soils with digestates with and  
623 without the organisms, and monitoring the gas kinetics in response to oxygen depletion, thus  
624 imitating the hot spots/hot moments of hypoxia/anoxia induced by digestates in soil  
625 (Kuzyakov and Blagodatskaya 2015). Since the isolates were raised by aerobic growth in  
626 autoclaved digestates, they would have to synthesize all denitrification enzymes in the soil,  
627 hence the synthesis of functional Nos was expected to be hampered by low pH (Liu et al 2014).  
628 The results for isolates **AS** and **AN** lend support to this (high  $I_{\text{N}_2\text{O}}$  in the soil with pH=5.5). **AN**  
629 was also dominating in the digestate enrichment culture, and in this case the organism had a  
630 strong and pH-independent effect on  $\text{N}_2\text{O}$  emission, plausibly due synthesis of Nos prior to  
631 incorporation into the soils.

632 In summary, we have demonstrated that a digestate from biogas production can be  
633 transformed into an effective agent for mitigating  $\text{N}_2\text{O}$  emission from soil, simply by allowing  
634 the right bacteria to grow to high cell densities in the digestate prior to fertilization. The  
635 technique is attractive because it can be integrated in existing biogas production systems, and

636 hence is scalable. If we manage to treat a major part of waste materials in agroecosystems by  
637 AD, the resulting digestates would suffice to treat a large share of total farmland, as illustrated  
638 by **Figure 1**. Estimation of the potential N<sub>2</sub>O-mitigation effect is premature, but the  
639 documented feasibility and the scalability of the approach warrant further refinement as well  
640 as rigorous testing under field condition. Our approach suggests one avenue for a much  
641 needed valorization of organic wastes (Peng and Pivato 2019) via anaerobic digestion. Future  
642 developments of this approach could extend beyond the scope of climate change mitigation  
643 and include the enrichment of microbes for pesticide- and other organic pollutant  
644 degradation (Sun et al 2018), plant growth promotion (Backer et al 2018) and inoculation of  
645 other plant symbiotic bacteria (Poole et al 2018).

646 **References**

647 Andalib M, Nakhla E, McIntee, Zhu J (2011) Simultaneous denitrification and methanogenesis (SDM):  
648 Review of two decades of research. *Desalination* 279:1-14. DOI:10.1016/j.desal.2011.06.018

649 Bakken LR, Frostegård Å (2020) Emerging options for mitigating N<sub>2</sub>O emissions from food  
650 production by manipulating the soil microbiota. *Current Opinion in Environmental Sustainability*  
651 47:89-94. <https://doi.org/10.1016/j.cosust.2020.08.010>

652 Backer R, Rokem JS, Ilangumaran G, Lamont J, Praslikova D, Ricci E, Subramnian S, Smith DL (2018)  
653 Plant growth-promoting rhizobacteria: context, mechanisms of action, and roadmap to  
654 commercialization of biostimulants for sustainable agriculture, *Front. Plant Sci.* 9:1473. doi:  
655 10.3389/fpls.2018.01473

656 Baral KR, Labouriau R, Olesen J, Petersen SO (2017) Nitrous oxide emissions and nitrogen use efficiency  
657 of manure and digestates applied to spring barley. *Agriculture Ecosystems & Environment* 239:188-  
658 198. DOI:10.1016/j.agee.2017.01.012

659 Bergaust L, Mao Y, Bakken LR, Frostegård Å (2010) Denitrification response patterns during the  
660 transition to anoxic respiration and posttranscriptional effects of suboptimal pH on nitrogen oxide  
661 reductase in *Paracoccus denitrificans*. *Applied and Environmental Microbiology* 76:6387-6396.  
662 DOI:10.1128/AEM.00608-10

663 Butterbach-Bahl K, Baggs EM, Dannenmann M, Kiese R, Zechmeister-Boltenstern S (2013) Nitrous  
664 oxide emissions from soils: how well do we understand the processes and their controls? *Philosophical  
665 Transactions of the Royal Society B* 368:20130122. DOI:10.1098/rstb.2013.0122

666 Cheng C, Shen X, Xie, H, Hu Z, Pavlostathis SG, Zhang J (2019) Coupled methane and nitrous oxide  
667 biotransformation in freshwater wetland sediment microcosms. *Science of the Total  
668 Environment* 648:916-922. DOI:10.1016/j.scitotenv.2018.08.185

669 Conthe M, Wittorf L, Kuenen JG, Kleerebezem R, van Loosdrecht MCM, Hallin S (2018) Life on N<sub>2</sub>O:  
670 deciphering the ecophysiology of N<sub>2</sub>O respiring bacterial communities in a continuous culture. *The  
671 ISME Journal* 12:1142–1153. DOI:10.1038/s41396-018-0063-7

672 D'Hondt K, Kostic R, McDowell R, Eudes F Singh BK, Sarkar S, Markakis B, Schelkle B, Maguin E,  
673 Sessitsch A (2021) Microbiome innovations for a sustainable future. *Nature Microbiology* 6:138-142.  
674 doi.org/10.1038/s41564-020-00857-w

675 Domeignoz-Horta LA, Putz M, Spor A, Bru D, Breuil MC, Hallin S, Philippot L (2016) Non-denitrifying  
676 nitrous oxide reducing bacteria – an effective N<sub>2</sub>O sink in soil. *Soil Biology and Biochemistry* 103:376-  
677 379. DOI:10.1016/j.soilbio.2016.09.010

678 Erisman JW, Sutton MA, Galloway J, Klimont Z, Winiwarter W (2008) How a century of ammonia  
679 synthesis changed the world. *Nature Geoscience* 1:636-639.

680 Eurostat (2017) Agri-environmental indicator – greenhouse gas emissions. ISSN 2443-8219,  
681 <https://ec.europa.eu/eurostat/statistics-explained/pdfscache/16817.pdf>

682 Fischer R, Gärtner P, Yeliseev A, Thauer RK (1992) N<sup>5</sup>-Methyltetrahydromethanopterin: coenzyme M  
683 methyltransferase in methanogenic archaeabacteria is a membrane protein. *Archives of Microbiology*  
684 158:208-217. DOI:10.1007/BF00290817

685 Foged HL, Flotats X, Blasi AB, Palatsi J, Magri A, Schelde KM (2011) Inventory of manure processing  
686 activities in Europe. Technical report No. I concerning “Manure Processing Activities in Europe” to the  
687 European Commission, Directorate-General Environment. 138.

688 Gao N, Shen WS, Kakuta H, Tanaka N, Fujiwara T, Nishizawa T, Takaya N, Nagamine T, Isobe K, Otsuka  
689 S, Senoo K (2016) Inoculation with nitrous oxide ( $N_2O$ )-reducing denitrifier strains simultaneously  
690 mitigates  $N_2O$  emission from pasture soil and promotes growth of pasture plants. *Soil Biology and*  
691 *Biochemistry* 97:83–91. DOI:10.1016/j.soilbio.2016.03.004

692 Gao N, Shen W, Camargo E, Shiratori Y, Nishizawa T, Isobe K, He X, Senoo K (2017) Nitrous oxide ( $N_2O$ )-  
693 reducing denitrifier-inoculated organic fertilizer mitigates  $N_2O$  emissions from agricultural soils.  
694 *Biology and Fertility of Soils* 53:885–898. DOI:10.1007/s00374-017-1231-z

695 Hallin S, Philippot L, Löffler RA, Jones CM (2018) Genomics and ecology of novel  $N_2O$ -reducing  
696 microorganisms. *Trends in Microbiology* 26:43–55. DOI:10.1016/j.tim.2017.07.003

697 Herrero M, Henderson B, Havlik P, Thornton PK, Conant RT, Smith P, Wirsén S, Hristov AN, Gerber  
698 P, Gill M, Butterbach-Bahl K, Valin H, Garnett T, Stehfest E (2016) Greenhouse gas mitigation  
699 potential in the livestock sector. *Nature Climate Change* 6:452–461. DOI:10.1038/nclimate2925

700 Holm-Nielsen JB, Al-Seadi T, Oleskowicz-Popiel P (2009) The future of anaerobic digestion and biogas  
701 utilization. *Bioresource Technology* 100:5478–5484. DOI:10.1016/j.biortech.2008.12.046

702 Hu HW, Chen D, He JZ (2015) Microbial regulation of terrestrial nitrous oxide formation:  
703 understanding the biological pathways for prediction of emission rates. *FEMS Microbiology Reviews*  
704 39:729–749. DOI:10.1093/femsre/fuv021

705 Kengen SWM, Mosterd JJ, Nelissen, RLH (1988) Reductive activation of the methyl-  
706 tetrahydromethanotering: coenzyme M methyl transferase from *Methanobacterium*  
707 *thermoautotrophicum* strain ΔH. *Archives of Microbiology* 150:405–412. DOI:10.1007/BF00408315

708 Kuzyakov Y, Blagodatskaya E (2015) Microbial hotspots and hot moments in soil: Concept & review.  
709 *Soil Biology and Biochemistry* 83:184–199. DOI:10.1016/j.soilbio.2015.01.025

710 Liu B, Frostegård Å, Bakken LR (2014) Impaired Reduction of  $N_2O$  to  $N_2$  in acid soils is due to a  
711 posttranscriptional interference with the expression of *nosZ*. *mBio* 5:e01383-14.  
712 DOI:10.1128/mBio.01383-14.

713 Lim YN, Frostegård Å, Bakken LR (2018) Nitrite kinetics during anoxia: The role of abiotic reactions  
714 versus microbial reduction. *Soil Biology and Biochemistry* 119:203–209.  
715 DOI:10.1016/j.soilbio.2018.01.006

716 Lu H, Chandran K, Stensel D (2014) Microbial ecology of denitrification in biological wastewater  
717 treatment. *Water Research* 64:237–254. DOI:10.1016/j.watres.2014.06.042

718 Lycus P, Bøthun KL, Bergaust L, Shapleigh JP, Bakken LR, Frostegård Å (2017) Phenotypic and genotypic  
719 richness of denitrifiers revealed by a novel isolation strategy. *The ISME Journal* 11:2219–2232.  
720 DOI:10.1038/ismej.2017.82

721 Lycus P, Soriana-Laguna, Kjos M, Richardson DJ, Gates AJ, Milligan DA, Frostegård Å, Bergaust L,  
722 Bakken LR (2018) A bet-hedging strategy for denitrifying bacteria curtails their release of  $N_2O$ .  
723 *Proceedings of the National Academy of Sciences USA* 115:11820–11825.  
724 DOI:10.1073/pnas.1805000115

725 Molstad L, Dörsch P, Bakken LR (2007) Robotized incubation system for monitoring gases (O<sub>2</sub>, NO,  
726 N<sub>2</sub>O, N<sub>2</sub>) in denitrifying cultures. *Journal of Microbiological Methods* 71:202-211.  
727 DOI:10.1016/j.mimet.2007.08.011

728 Molstad L, Dörsch P, Bakken LR (2016) Improved robotized incubation system for gas kinetics in  
729 batch cultures. *Researchgate*. DOI:10.13140/RG.2.2.30688.07680

730 Mania D, Wolily K, Degefu T, Frostegård Å (2020) A common mechanism for efficient N<sub>2</sub>O reduction in  
731 diverse isolates of nodule-forming bradyrhizobia. *Environmental Microbiology* 22:17-31.  
732 DOI:10.1111/1462-2920.14731

733 Meyer A, Ehimen E, Holm-Nielsen J (2018) Future European biogas: Animal manure, straw and grass  
734 potentials for a sustainable European biogas production. *Biomass and Energy* 111:154-164.  
735 DOI:10.1016/j.biombioe.2017.05.013

736 Nadeem S, Bakken LR, Frostegård Å, Gaby JC, Dörsch P (2020) Contingent effects of liming on N<sub>2</sub>O-  
737 emissions driven by autotrophic nitrification. *Frontiers in Environmental Science* 8:598513.  
738 DOI:10.3389/fenvs.2020.598513

739 Peng W, Pivato A (2019) Sustainable Management of Digestate from the Organic Fraction of Municipal  
740 Solid Waste and Food Waste Under the Concepts of Back to Earth Alternatives and Circular Economy.  
741 *Waste Biomass Valor* (2019) 10:465–481. DOI 10.1007/s12649-017-0071-2

742 Poole P, Ramachandran V, Terpolilli J (2018) Rhizobia: from saprophytes to endosymbionts *Nature*  
743 *Reviews Microbiology* 16:291-303. doi:10.1038/nrmicro.2017.171

744 Qu Z, Bakken LR, Frostegård Å, Bergaust L (2016) Transcriptional and metabolic regulation of  
745 denitrification in *Paracoccus denitrificans* allows low but significant activity of nitrous oxide reductase  
746 under oxic conditions. *Environmental Microbiology* 18:2951-2963. DOI:10.1111/1462-2920.13128

747 Richter M, Rosselló-Móra R (2009) Shifting the genomic gold standard for the prokaryotic species  
748 definition. *Proceedings of the National Academy of Sciences USA* 106:19126-19131.  
749 DOI:10.1073/pnas.0906412106

750 Russenes AL, Korsæth A, Bakken LR, Dörsch P (2016) Spatial variation in soil pH controls off-season  
751 N<sub>2</sub>O emission in an agricultural soil. *Soil Biology and Biochemistry* 99:36-46.  
752 DOI:10.1016/j.soilbio.2016.04.019

753 Sanford RA, Wagner DD, Wu Quingzhong, Chee-Sanford JC, Thomas SH, Cruz-Garzia C, Rodrigues G,  
754 Massol-Deya A, Krishnani KK, Ritalahti KM, Nissen S, Konstantinidis KT, Löffler FE (2013) Unexpected  
755 nondenitrifier nitrous oxide reductase gene diversity and abundance in soils. *Proceedings of the*  
756 *National Academy of Sciences USA* 109:19709-19714. DOI:10.1073/pnas.1211238109

757 Scarlat N, Dallemand JF, Fahl F (2018) Biogas: Developments and perspectives in Europe. *Renewable*  
758 *Energy* 129:457-472. DOI:10.1016/j.renene.2018.03.006

759 Shapleigh JP (2013) Denitrifying Prokaryotes. in: Rosenberg E, DeLong EF, Lory S, Stackebrandt E,  
760 Thompson F (editors). *Prokaryotes - Prokaryotic Physiology and Biochemistry* (Springer Berlin,  
761 Heidelberg, 405–425). DOI:10.1007/978-3-642-30141-4\_71

762 Schink B (1997) Energetics of syntrophic cooperation in methanogenic degradation. *Microbiology*  
763 and *Molecular Biology Reviews* 61:262-280. DOI:1092-2172/97/\$04.0010

764 Snyder CS, Davidson EA, Smith P, Venterea RT (2014) Agriculture: sustainable crop and animal  
765 production to help mitigate nitrous oxide emissions. *Current Opinions in Environmental Sustainability*  
766 9:10:46-54.

767 Song X, Liu M, Ju X, Gao B, Su F, Chen X, Rees RM (2018) Nitrous oxide emissions increase  
768 exponentially when optimum nitrogen fertilizer rates are exceeded in the North China Plain.  
769 *Environmental Science and Technology* 52:12504–12513. DOI:10.1021/acs.est.8b03931

770 Sutton M, Erisman W, Leip A, vanGrinsven H, Winiwarter W (2011) Too much of a good thing. *Nature*  
771 472: 159-161.

772 Spiro S (2016) Regulation of denitrification. (Chapter 13) in: Isabel M, José JGM, Sofia RP, Luisa BM  
773 (editors). *RSC Metallobiology Series 9: Matalloenzymes in denitrification* (Royal Society of Chemistry  
774 Cambridge, UK, 312-331). <https://doi.org/10.1039/9781782623762-00312>

775 Stams AJM, Elferink SJWHO, Westermann P (2003) Metabolic Interactions Between Methanogenic  
776 Consortia and Anaerobic Respiring Bacteria. in: Ahring BK (editors). *Biomethanation I. Advances in*  
777 *Biochemical Engineering/Biotechnology*, vol 81 (Springer Berlin, Heidelberg). DOI: 10.1007/3-540-  
778 45839-5\_2

779 Stenmarck AA, Jensen C, Quested T, Moates G (2016) Estimates of European food waste levels,  
780 Report of the project FUSIONS (contract number: 311972) granted by the European Commission  
781 (FP7). DOI:10.13140/RG.2.1.4658.4721

782 Sun S, Sidhu V, Rong Y, Zheng Y (2018) Pesticide Pollution in Agricultural Soils and Sustainable  
783 Remediation Methods: a Review. *Current Pollution Reports* 4:240-250. doi.org/10.1007/s40726-018-  
784 0092-x

785 Tian H, et al (2020) A comprehensive quantification of global nitrous oxide sources and sinks. *Nature*  
786 586:248-255. DOI:10.1038/s41586-020-2780-0

787 Valenzuela El, Padilla-Loma C, Gómez-Hernández N, López-Lozano NE, Casas-Flores S, Cervantes FJ  
788 (2020) Humic substances mediate anaerobic methane oxidation linked to nitrous oxide reduction in  
789 wetland sediments. *Frontiers in Microbiology* 11:587. DOI:10.3389/fmicb.2020.00587

790 Vaccaro BJ, Thorgersen MP, Lancaster WA, Price MN, Wetmore KM, Poole FL, Deutschbauer A, Arkin  
791 AP, Adams MWW (2016) Determining roles of accessory genes in denitrification by mutant fitness  
792 analyses. *Applied and Environmental Microbiology* 82:51-61. DOI:10.1128/AEM.02602-15

793 Yoon S, Nissen S, Park D, Sanford RA, Löffler FE (2016) Nitrous oxide reduction kinetics distinguish  
794 bacteria harboring Clade I NosZ from those harboring Clade II NosZ. *Applied and Environmental*  
795 *Microbiology* 82:3793-3800. doi:10.1128/AEM.00409-16.

796 Zumft WG (1997) Cell biology and molecular basis of denitrification. *Microbiology and Molecular*  
797 *Biology Reviews* 61:533-616. DOI:1092-2172/97/\$04.0010